

Bipolaron: The Stable Charged Species in *n*-Doped *p*-Sexiphenyl

N. Koch,^{*,†} A. Rajagopal,[‡] J. Ghijsen,[‡] R. L. Johnson,[§] G. Leising,[†] and J.-J. Pireaux[‡]

Institut für Festkörperphysik, TU-Graz, A-8010 Graz, Austria, Laboratoire Interdisciplinaire de Spectroscopie Electronique, Facultés Universitaires Notre-Dame de la Paix, B-5000 Namur, Belgium, and Institut für Experimentalphysik, Universität Hamburg, D-22761 Hamburg, Germany

Received: April 26, 1999; In Final Form: November 23, 1999

The change in the valence electronic structure of thin films of the electroluminescent material *p*-sexiphenyl (6P) has been investigated as a function of the deposition of an alkaline earth metal under ultrahigh vacuum conditions. This was done by in situ evaporation of increasing amounts of calcium onto the 6P film and recording the photoemission spectra. Two different substrates for the 6P films were used, namely Au and Ca. New emissions within the formerly empty energy gap of the pristine organic material were observed upon the metal deposition for both substrates. For 6P/Au this was accompanied by a significant shift of the Fermi level (E_F) toward lower binding energy for increasing amounts of Ca. For low metal coverage the density of occupied valence states (DOVS) of the intragap emission was observed at E_F , whereas for higher amounts of Ca coverage no DOVS are observed at E_F . Commonly, this would be interpreted that first polarons (radical anions) are formed, and later on bipolarons (dianions) for higher Ca concentration. In contrast, on the basis of the different experimental findings when Ca was used as substrate and a line shape analysis of the intragap emission, we conclude that in 6P bipolarons are formed throughout all doping levels.

1. Introduction

Conjugated organic materials attract much scientific interest because they exhibit properties directly applicable in industrial products. These properties include efficient photoluminescence, electroluminescence,^{1–5} and high electrical conductivity under certain conditions,⁶ the potential products being indicators, flat panel displays,^{7,8} and field-effect transistors.^{9,10} Since metal-like conductivity was demonstrated with doped polyacetylene,¹¹ a huge effort was made to elucidate the electronic nature of charge transport in conjugated polymers. Additional interest for this issue stems from the need for efficient charge injection and transport in conjugated materials that are used in organic light emitting devices (OLEDs). Charge transport in these nondegenerate ground-state systems occurs via molecules with an excess or a deficiency of electrons. These anionic and cationic molecules are then discussed within the framework of negative and positive polarons (one extra charge) or bipolarons (two extra charges), respectively. It is commonly accepted^{12–14} that the electron energy levels associated with these species are located within the forbidden energy gap of the neutral organic semiconductor. As polarons possess a half-filled highest occupied molecular orbital (HOMO), their energy position is predicted to be destabilized compared to the one of the bipolaron, which has a completely filled HOMO. Consequently, the electronic states of the bipolaron are found deeper in the energy gap than those of polarons, as shown in Figure 1, where the expected position of the Fermi level for a homogeneous ensemble of molecules is also indicated by a dotted line. From this figure one can conclude that a density of valence states (DOVS) should be observable at E_F for polarons, and the DOVS are expected to lie well above E_F for bipolarons.

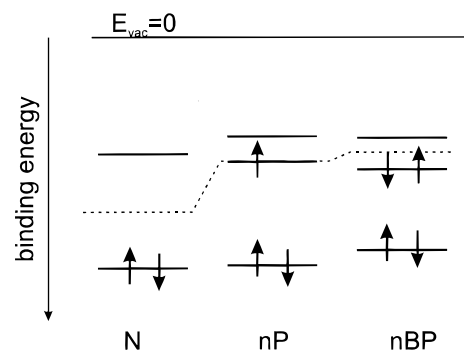


Figure 1. Schematic energy-level diagram for a nondegenerate ground-state conjugated organic molecule in the neutral state (N), with one excess electron (negative polaron, nP) and with two excess electrons (negative bipolaron, nBP). The binding energy scale only reflects the general trend in such systems. The dashed line indicates the expected position of the Fermi energy for a homogeneous assemble of the individual species.

One method to investigate experimentally the intragap states that result from excess charges on the conjugated molecule is to deposit a dopant, often alkali or alkaline earth metals that are prone to donate electrons, onto a thin film of the organic material and to analyze the consequent changes in the ultraviolet photoemission spectra. Photoemission spectroscopy enables the determination of binding energies of occupied electronic states, as well as the position of the Fermi level. The results of such an experiment are presented here, with *p*-sexiphenyl (6P) as the conjugated system and calcium as the dopant. 6P is a wide band-gap (3.1 eV) electroluminescent oligomer of poly(paraphenylene), which can be used to prepare efficient blue light emitting devices.^{15,16} Ca is one of the low work function metals that is commonly used as a cathode material in OLEDs. It has been demonstrated that if Ca is used as the electron-injecting contact in OLEDs with poly(*p*-phenylenevinylene) (PPV) as the

[†] Institut für Festkörperphysik.

[‡] Universitaires Notre-Dame de la Paix.

[§] Universität Hamburg.

active material, the performance of the device is very sensitive to the presence of oxygen at the metal/polymer interface.¹⁷ Without the formation of a calcium oxide interface layer, the performance is rather poor. The reason seems to be that in the case of pure Ca the metal diffuses significantly into the active material and dopes the polymer in the interface region. In an ultraviolet photoemission spectroscopy (UPS) study of Ca on PPV the newly emerging intragap states were attributed to the formation of negative bipolarons,^{18,19} even at very low concentrations of Ca on the polymer surface. On the other hand, in another experiment rubidium was deposited onto PPV and a model oligomer thereof,²⁰ and evidence was found that for the low doping regime polarons are formed, whereas for higher doping levels the intragap emissions are attributed to bipolarons. This assignment was based on the observation that the Fermi level was located at the position of the observed new DOVS for the low Ca concentration and that E_F was found below this DOVS position at higher doping levels. This leads to an interpretation in terms of a polaron–bipolaron transition. A similar experimental result was obtained by Steinmueller et al.²¹ When Cs was evaporated onto a bithiophene thin film, the evolution of two energetically well-separated intragap emissions on the low binding energy side was clearly observed. Their relative intensities were strongly dependent on the amount of Cs present on the sample, clearly indicating a transition from one doping regime to another, presumably polarons and bipolarons. One drawback of these experimental observations is that, even in the polaron domain, E_F is located below any DOVS, which is attributed to an incomplete screening of the hole left behind by the emitted photoelectron. Yet, these observations are to be interpreted as a polaron–bipolaron transition.

In our UPS study of Ca on 6P we obtained spectra similar to the above-mentioned results. However, we propose an alternative interpretation to the polaron–bipolaron transition. This is based on the finding that the position of the Fermi level in the doped sample strongly depends on the work function of the pristine organic material, and on a line shape analysis of the new intragap emission.

2. Experimental Section

The UPS experiments were performed at the FLIPPER II beamline in Hasylab at DESY.²² The evaporations of 6P and Ca were performed in situ, at a pressure lower than 3×10^{-9} mbar in the preparation chambers. Gold-coated silicon wafers were cleaned by Ar-ion sputtering in situ before evaporating 6P (purchased from Tokyo Chemicals Ltd., Japan) from a pinhole source. An alternative substrate for 6P was a thick Ca film, evaporated onto a cleaned Au-coated Si wafer. The clean Au and Ca films were used to determine the position of the Fermi energy. The thickness of 6P on Au was 400 Å and on Ca 110 Å, as monitored by a quartz microbalance. After having calibrated the Ca evaporation source using a quartz microbalance, Ca was evaporated onto the 6P films in a stepwise manner, the initial steps chosen to be extremely small. After each consecutive step, without breaking the UHV, the samples were transferred to the analysis chamber in order to record the spectra, where the pressure was below 2×10^{-10} mbar throughout the experiment. The samples were biased negatively with respect to the electron spectrometer in order to enable the determination of binding energies with respect to the vacuum level. A photon energy of 32 eV was chosen because of the high photoelectron cross-section for the valence region of 6P at this value.²³ Great care was taken to keep the photon energy constant, and to guarantee that the 6P films do not exhibit any charging effects.

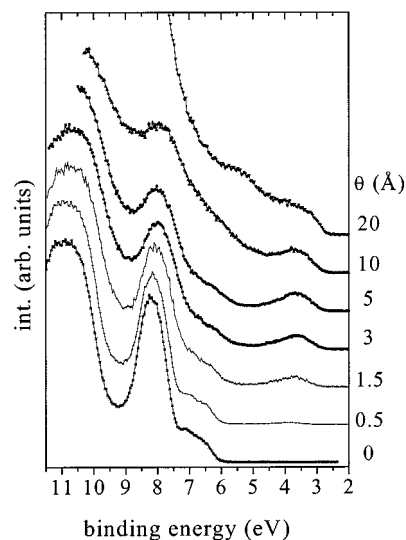


Figure 2. UPS spectra of a 6P thin film with increasing amounts of Ca (θ) deposited on it. The binding energy is given with respect to the vacuum level, set at zero.

3. Results

The valence electronic region of the pristine 6P film on Au is presented as the lowest curve in Figure 2. The binding energies in this figure are given with respect to the vacuum level ($E_{B,vac}$), set at zero. In UPS the kinetic energies of the photoelectrons are measured (E_{kin}), and the binding energies with respect to the vacuum level are obtained from the following equation, if the sample is biased negatively with respect to the electron spectrometer during the measurements: $E_{B,vac} = h\nu - (E_{kin} - E_{kin,CO})$; where $h\nu$ is the incident photon energy and $E_{kin,CO}$ is the kinetic energy of the low kinetic energy secondary electron cutoff.

The first ionization potential of 6P can be determined directly from the width of the energy distribution curve (EDC) of the UP spectrum. The EDC is obtained by a linear extrapolation of the HOMO, and the onset of the secondary electron cutoff toward the background. We find this value to be 6.1 eV for the pristine 6P films, in good agreement with earlier reported values of 5.95²⁴ and 6.1 eV,²⁵ respectively.

Ca was deposited stepwise onto this clean 6P/Au film, and the photoelectron spectra recorded after each subsequent step. The so obtained valence electronic spectra and a close-up of the frontier orbitals are presented in Figures 2 and 3, respectively. The first deposition step of Ca on 6P was chosen to be extremely small, i.e., 0.05 Å. This corresponds roughly to one Ca atom per 100 6P molecules, assuming standing molecules and no Ca diffusion. The following Ca depositions were done with an increasingly larger step size. In the survey plot (Figure 2) one can observe that after having deposited 1.5 Å Ca on the 6P surface, new occupied electronic states appear in the formerly empty gap with significant intensity. The new low binding energy emission is centered at 3.75 eV; the binding energy for the other new state cannot be estimated accurately, since it is located only little below the HOMO peak of the pristine 6P. These emissions continue to become more intense for higher coverage. Additionally, after 10 Å of Ca coverage, the overall spectral features of 6P become broader and the whole spectrum shifts toward lower binding energy by about 0.2 eV (with respect to the pristine organic film). With 20 Å Ca, and more, the emission from Ca is dominating the spectrum. However, it is not yet in a metallic state, since no Fermi edge can be observed. Here it must be noted that 20 Å is the coverage indicated by

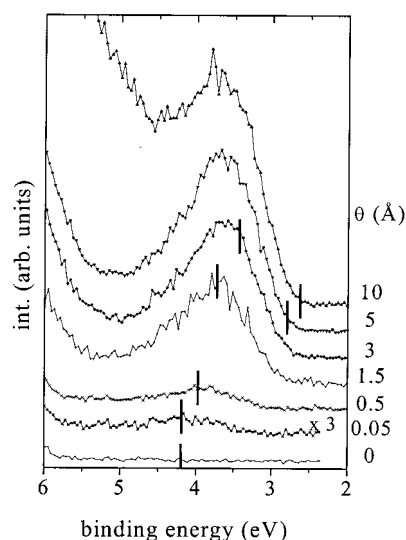


Figure 3. Close-up of the low binding energy region of Figure 2. The bar indicates the position of the Fermi level as determined in the UPS experiment.

the microbalance. This does not mean that a uniform film of this thickness is formed. A close-up of the “gap region” of 6P (Figure 3) provides further insight into the evolution of both the intensity and energy position of the newly occupied electronic states due to the deposition of Ca on the organic surface. A bar indicates the position of the Fermi energy for each spectrum. Now, even at only 0.05 Å Ca coverage the upper new electronic state centered at roughly 3.9 eV becomes visible (poor signal/noise ratio). With increasing coverage this emission grows in intensity, and gradually shifts to reach its final binding energy of 3.6 eV at a coverage of 1.5 Å. Throughout the experiment, up to 10 Å Ca on 6P, the line shape of this emission does not change. The increasing amount of Ca, leading to the new intragap states, has a significant effect on the position of the Fermi energy (E_F) of the 6P/Au sample. For the pristine 6P film E_F is found at 4.2 eV from the vacuum level (i.e., the work function), or 1.9 eV below the HOMO onset. This determination follows from the measured position of E_F for a clean Au surface, and the above equation. After the first deposition of Ca (0.05 Å) the work function of the sample is decreased by a mere 0.05 eV. Any further deposition of the metal causes a continuous shift of E_F to lower energies, reaching a final value of 2.6 eV,

which is achieved at 10 Å coverage. Since at all stages the new emission in the former energy gap is present and it only shifts by roughly 0.3 eV, E_F is initially found within this peak, and then gradually moves out of it, until it is found well below any density of occupied states for coverages higher than 5 Å. The metallic Fermi edge of Ca becomes visible only for more than 50 Å Ca coverage, and we measure a work function value of 3.2 eV for this metallic film.

In another set of experiments, a thin film of 6P was evaporated onto metallic Ca, and subsequently covered with increasing amounts of Ca. Figure 4a shows the photoemission spectra of this series. The Fermi level is chosen as the energy reference, set at zero. For comparison, spectra of the series with Au as substrate are also shown in Figure 4b, on the same energy scale and for similar Ca coverage. We find that when 6P is evaporated onto Ca, E_F is located 2.7 eV below the HOMO onset (i.e., a work function of 3.4 eV). This must be attributed to a different interaction of the first 6P monolayer with metallic Ca as compared to metallic Au. In ref 26 it is shown in detail that 6P physisorbs on Au. We observed that UP spectra of thin 6P films (20 Å and less) on Ca (spectra not shown) exhibit marked differences compared to thicker ones, or those formed on Au. This clearly indicates a strong chemical interaction between 6P and a metallic Ca surface. The nature of the interaction of 6P with metallic Ca is not within the scope of this paper. However, the 6P molecules in intimate contact with the Ca surface determine the position of E_F , and due to the low intrinsic defect concentration in 6P this position is pinned also for the thicker film, as is to be expected for large band-gap materials.²⁷ Since for 6P/Ca the work function of the pristine 6P is already small, the shift of the Fermi level for increasing Ca deposition shows a noticeably different behavior than when Au served as substrate. Even at 0.5 Å Ca coverage E_F is found well below the new doping-induced DOVS, and for increasing Ca deposition the whole spectrum shifts little toward higher binding energies (cf. Figure 4a). As one can see from Figure 4b, when the work function of the pristine 6P film is higher (Au as substrate) the new DOVS are found at E_F for even higher coverage than 3 Å. The consequences of these findings will be discussed in the second part of the following section.

4. Discussion

As outlined in the Introduction, a negative polaron (nP) is formed due to the filling of the former LUMO of the organic

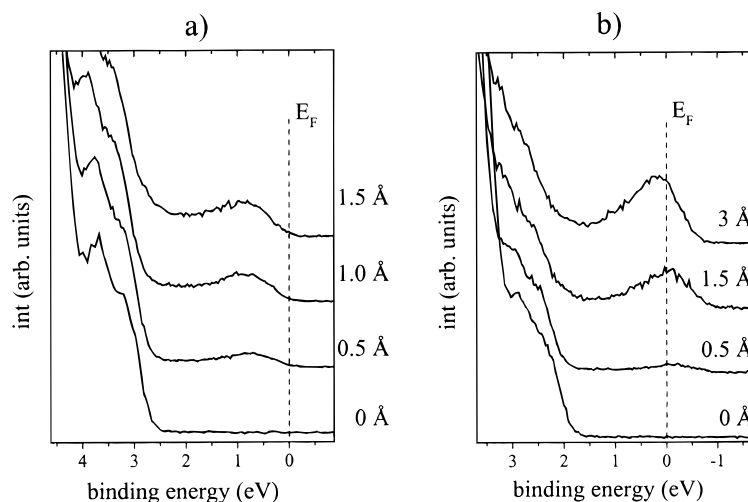


Figure 4. Close-up of the low binding energy region of Ca deposited onto (a) 6P/Ca and (b) 6P/Au. The binding energy is given with respect to the Fermi level, set at zero.

molecule with one electron. This leads to a stabilization (increased binding energy) of this newly occupied state, and a destabilization (lower binding energy) of the former HOMO. Due to the fact that this molecule now has a half-filled orbital, there should be a DOVS at the Fermi level, by definition.^{12–14} If a second electron is added to the molecule, the half-filled orbital will become a completely filled one and E_F will be expected to be found between this orbital and the new LUMO (LUMO+1 in the neutral molecule), well below any DOVS. For this negative bipolaron (nBP) the new completely filled orbital is stabilized even more than in the case of the nP, and the opposite holds for the former HOMO; i.e., it would be more destabilized.

First we consider the experiment with Au as substrate. From the perspective of the movement of the Fermi level alone, one could already conclude that we observe negative polarons during the initial stages of Ca exposure, since E_F is found well within occupied electronic states (see Figure 3.). For a higher amount of Ca on the 6P surface E_F moves toward lower binding energy and is found well below the new intragap emission, indicating that the observed species are negative bipolarons. What we observe then could be interpreted as a transition from nP's in our sample with low Ca concentration, toward a situation with only nBP's being present at high coverage with Ca, passing through intermediate stages where nP's and nBP's are present at the same time. Nevertheless, there are considerations, which make the validity of a simple nP–nBP transition questionable in the case of doping 6P with Ca.

The above-mentioned rigid shift of the whole spectrum by about 0.2 eV when going from the pristine 6P/Au film to a high Ca coverage can be explained by a more efficient screening of the hole left behind after the photoemission of an electron, due to the doping of the organic material. This effect is already completed after 1.5 Å Ca has been deposited (cf. Figure 2.). Another possible way of plotting the experimental curves, and thereby taking account of the change in the hole screening efficiency, is to align them with respect to the maximum of the localized π -state,^{23,24} which is found at a binding energy of 8.2 eV for the pristine film. This method is also justified in the first approximation by calculations performed on various neutral, singly and doubly negatively charged conjugated systems,²⁸ where it was found that the binding energy of this peak is least affected by doping. We say in a first approximation, because one must bear in mind that in these calculations any effects due to the presence of counterions, which may result in a different situation in the actual experiment, are neglected. Figure 5 presents the “gap region” from Figure 2 plotted in this way, and additionally, the spectra are normalized to the maximum of the new low binding energy emission due to the Ca deposition. In this plot no significant changes of the new emission, either in position or in line shape, can be observed when going from low Ca coverage (DOVS at E_F) to high Ca coverage (E_F below DOVS; 5 Å Ca and more). The new HOMO emission from a nP is expected to appear below the emission from the new HOMO of a nBP. Therefore a transition from nP to nBP should result in the observation of one state growing first (nP), the subsequent appearance of a new emission at higher binding energy (nBP) with increasing dopant concentration, and finally—for the highest doping levels—continuous growth of the nBP while the nP should disappear. As a consequence, if one assumes the predicted different binding energy of nP– and nBP–HOMO, this implies that this new intragap emission stems from the same electronic species, throughout the doping experiment.

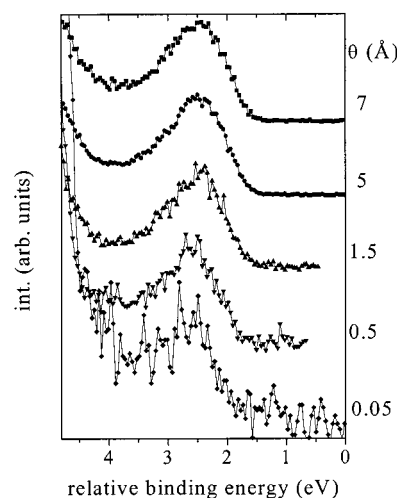


Figure 5. Representative curves from Figure 3, aligned on the energy scale by the peak of the localized π -state and normalized to the intensity of the low binding energy intragap emission.

We assign this new emission to a bipolaron for the following reasons. Since for high Ca coverage the Fermi level is found below any occupied electronic states, it is reasonable to assume that this emission is coming from the HOMO of negative bipolarons. The experimentally determined shift of E_F and the observation of DOVS at E_F for low coverages for 6P/Au must have another origin. This becomes evident when investigating the spectral shifts observed for 6P/Au and 6P/Ca. By comparing the position of E_F relative to the new doping-induced emissions for the two different experiments shown in Figure 4a,b one must conclude that the presence of DOVS at E_F in doped wide band-gap conjugated materials does not automatically imply the presence of polarons. When up to 3 Å Ca are deposited onto 6P/Au, a finite DOVS is observed at E_F , and the presence of nP's could be concluded. However, for similar doping concentrations *no* DOVS are found at the Fermi energy when Ca is used as substrate. It appears that for 6P/Ca E_F of the pristine film is already very close to the position obtained for high doping levels (5 Å Ca, and more for 6P/Au). Already at very low Ca coverage E_F accommodates a position corresponding to the one expected for nBP's. The observation of E_F within the new DOVS when Au is used as substrate must be attributed to the way the Fermi level is determined in photoemission spectroscopy for an inhomogeneous sample. Currently, experiments are being performed to elucidate the exact nature of this phenomenon. The conclusion from our experimental results is that from the very beginning in both doping series negative bipolarons are formed. Only the shift of E_F is different, due to the variation of initial work functions of 6P/Au and 6P/Ca. This is supported by the absence of a change in the line shape of the new intragap emission throughout all doping levels. Additionally the formation of nBP's is expected to be energetically favorable compared to the formation of nP's. Here we also note that in a solid-state cyclovoltammetry experiment performed with 6P the first observed reduction wave was due to a two-electron transfer, indicating the formation of dianions (bipolarons).²⁹

5. Conclusion

Ultraviolet photoelectron spectroscopy has been used to investigate the formation of negatively charged species in electroluminescent *p*-sexiphenyl. To do this, thin films of 6P (on Au and Ca, respectively) were exposed to increasing amounts of Ca in vacuo. The resulting changes in the valence

electronic region after alkaline-earth metal deposition were followed by ultraviolet photoelectron spectroscopy. The deposition of calcium led to new electronic emissions within the forbidden energy gap of neutral 6P. The intensity of the low binding energy emission, which is due to filling the former LUMO of 6P with electrons, is clearly correlated to the amount of Ca present on the sample. For 6P/Au a large shift of the Fermi level toward lower binding energy is observed. While for low Ca coverage E_F is found right within the new intragap emission, E_F gradually moves out of the DOVS for higher coverage. When Ca is used as the substrate, the work function of the pristine 6P film is smaller by 0.9 eV compared to that of 6P/Au. The reason for this is the pinning of E_F at the 6P/Ca interface due to a strong chemical interaction. When Ca is deposited onto 6P/Ca the same new intragap emissions are observed as for 6P/Au, but *no* DOVS is observed at E_F , regardless of the doping concentration. As also the line shape of the low binding energy emission does not change for all doping levels, we do not assign the observed phenomenon to a polaron–bipolaron transition; instead, we conclude that bipolarons are formed from the very beginning of Ca deposition. These results will have a severe impact on the understanding and description of charge transport in doped conjugated systems.

Acknowledgment. The synchrotron work was supported by the TMR-contract ERBFMGECT950059 of the European Community. A.R. acknowledges the financial support of the Interuniversity Research Projects (PAI/IUA) on “Sciences of Interfacial and Mesoscopic Structures and Materials Characterization” sponsored by the Belgian Prime Minister’s Office (Federal Services for Scientific, Technical and Cultural Affairs). J.G. is supported by the Belgian NFSR. R.L.J.’s research is funded by BMBF projects BMBF 05 622 GUA and BMBF 05 SB8 GUA.

References and Notes

- (1) Tang, C. W.; van Slyke, S. A. *Appl. Phys. Lett.* **1987**, *51*, 913.
- (2) Burroughes, J. H.; Bradley, D. D. C.; Brown, A. R.; Marks, R. N.; Mackey, K.; Friend, R. H.; Burns, P. L.; Holmes, A. B. *Nature* **1990**, *347*, 539.
- (3) Braun, D.; Heeger, A. J. *Appl. Phys. Lett.* **1991**, *58*, 1982.
- (4) Ohmori, V.; Uchida, M.; Muro, K.; Yoshino, K. *Jpn. J. Appl. Phys.* **1991**, *30*, L1941.
- (5) Grem, G.; Leditzky, G.; Ullrich, B.; Leising, G. *Adv. Mater.* **1992**, *4*, 36.
- (6) Menon, R.; Yoon, C. O.; Moses, D.; Heeger, A. J. In *Handbook of Conducting Polymers*, 2nd ed.; Skotheim, T., Elsenbaumer, R., Reynolds, J., Eds.; Dekker: New York, 1997.
- (7) Tang, C. W.; Williams, D. J.; Chang, J. C. U.S. Patent 5294870, 1994.
- (8) Tasch, S.; Brandstätter, C.; Meghdadi, F.; Leising, G.; Froyer, G.; Athouel, L. *Adv. Mater.* **1997**, *33*, 9.
- (9) Horowitz, G.; Fichou, D.; Peng, X.; Shu, Z.; Garnier, F. *Solid State Commun.* **1989**, *72*, 381.
- (10) Paloheimo, J.; Kuivalainen, P.; Stubb, H.; Vuorimaa, E.; Yli-Lahti, P. *Appl. Phys. Lett.* **1990**, *56*, 1157.
- (11) Heeger, A. J.; Kivelson, S.; Schrieffer, J. R.; Su, W. P. *Rev. Mod. Phys.* **1988**, *60*, 781.
- (12) Baeriswyl, D.; Campbell, D. K.; Mazumdar, S. In *Conjugated Conducting Polymers*; Kiess, H., Ed.; Springer Series in Solid-State Sciences Vol. 102; Springer: Berlin, 1992.
- (13) Conwell, E. M.; Mizes, H. A. *Phys. Rev. B* **1991**, *44*, 937.
- (14) Salaneck, W. R.; Brédas, J. L. *Synth. Met.* **1994**, *67*, 15.
- (15) Graupner, W.; Grem, G.; Meghdadi, F.; Paar, Ch.; Leising, G.; Scherf, U.; Müllen, K.; Fischer, W.; Stelzer, F. *Mol. Cryst. Liq. Cryst.* **1994**, *256*, 549.
- (16) Leising, G.; Tasch, S.; Graupner, W. In *Handbook of Conducting Polymers*, 2nd ed.; Skotheim, T., Elsenbaumer, R., Reynolds, J., Eds.; Dekker: New York, 1997.
- (17) Bröms, P.; Birgersson, J.; Johansson, N.; Lögdlund, M.; Salaneck, W. R. *Synth. Met.* **1995**, *74*, 179.
- (18) Lazzaroni, R.; Lögdlund, M.; Calderone, A.; Brédas, J. L. *Synth. Met.* **1995**, *71*, 2159.
- (19) Salaneck, W. R.; Brédas, J. L. *Adv. Mater.* **1996**, *8*, 48.
- (20) Iucci, G.; Xing, K.; Lögdlund, M.; Fahlman, M.; Salaneck, W. R. *Chem. Phys. Lett.* **1995**, *244*, 139.
- (21) Steinmüller, D.; Ramsey, M. G.; Netzer, F. P. *Phys. Rev. B* **1993**, *47*, 1323.
- (22) Johnson, R. L.; Reichardt, J. *Nucl. Instrum. Methods* **1983**, *208*, 719.
- (23) Narioka, S.; Ishii, H.; Edamatsu, K.; Kamiya, K.; Hasegawa, S.; Ohta, T.; Ueno, N.; Seki, K. *Phys. Rev. B* **1995**, *52*, 2362.
- (24) Seki, K.; Karlsson, U. O.; Engelhardt, R.; Koch, E. E.; Schmidt, W. *Chem. Phys.* **1984**, *91*, 459.
- (25) Koch, N.; Yu, L. M.; Parenté, V.; Lazzaroni, R.; Johnson, R. L.; Leising, G.; Pireaux, J. J.; Brédas, J. L. *Adv. Mater.* **1998**, *10*, 1038.
- (26) Oji, H.; Ito, E.; Furuta, M.; Kajikawa, K.; Ishii, H.; Ouchi, Y.; Seki, K. *J. Electron. Spectrosc. Relat. Phenom.* **1999**, *101–103*, 517.
- (27) Malaske, U.; Tegenkamp, C.; Henzler, M.; Pfnür, H. *Surf. Sci.* **1998**, *408*, 237.
- (28) Lögdlund, M.; Dannetun, P.; Fredriksson, C.; Salaneck, W. R.; Brédas, J. L. *Phys. Rev. B* **1996**, *53*, 16327.
- (29) Meerholz, K.; Heinze, J. *Angew. Chem., Int. Ed. Engl.* **1990**, *29*, 692.